FLICKERING OF A NICOTINIC ION CHANNEL TO A SUBCONDUCTANCE STATE

ANTHONY AUERBACH AND F. SACHS
Department of Biophysics, State University of New York, Buffalo, New York 14214

ABSTRACT Nicotinic acetylcholine channels show bursts of activity where open channel currents are separated from each other by short closed periods called flickers. These flickers presumably represent transitions from the open state to the state preceding the first opening of a burst (doubly liganded, closed state). Using tissue cultured chick pectoral muscle, we have examined the amplitude distribution of flickers. Of those events sufficiently long to permit accurate measurement of the amplitude (~25% of all flickers), approximately two-thirds had a mean current equal to 10% of the fully open channel. The remaining one-third did appear to close completely. The subconducting flicker state is not a requisite step preceding channel opening. We conclude that there are three types of flicker events: a short event (time constant ~0.1 ms) whose current distribution is uncertain and two longer events (time constant ~1 ms), one of which has a current ~10% of the main open state and the other of which has a current indistinguishable from zero. In contrast, the amplitude of flickers induced by the local anesthetic QX-222 is indistinguishable from zero.

INTRODUCTION

In the traditional model for the activation of nicotinic channels, acetylcholine binds to closed channels that then undergo a transition to an open conformation (del Castillo and Katz, 1957). Since dose-response studies indicate that open channels usually have at least two agonist molecules bound (Dionne et al., 1978; Dreyer et al., 1978), a minimal model would have three closed (R, AR, and A_2R) and one open state (A_2R^*), where A represents agonist and R, the receptor

$$2A + R \underset{k_{d_1}}{\overset{k_{a_1}}{\rightleftharpoons}} A + AR \underset{k_{d_2}}{\overset{k_{a_2}}{\rightleftharpoons}} A_2R \underset{\alpha}{\overset{\beta}{\rightleftharpoons}} A_2R^*. \qquad (1)$$

This model predicts that it is possible for one or more interconversions between the doubly liganded open and closed states to occur before dissociation of agonist (Colquhoun and Hawkes, 1977, 1981; Sakmann and Adams, 1979). The probability of such interconversions is determined by the ratio of the channel opening rate (β) to the rate of agonist dissociation k_{d_2}. In single channel recordings, currents would then appear in bursts with short transitions to the nonconducting state separating events characteristic of the open time of a single channel.

We will call short transitions from the open state toward the zero conductance level flickers. Flickers, in the absence of extrinsic blocking agents, were first reported by Nelson and Sachs (1979) in suberyldicholine-activated channels in cultured chick skeletal muscle. More recently, Colquhoun and Sakmann (1981), Dionne and Leibowitz (1982), and Nelson and Sachs (1982) have analyzed flicker kinetics for nicotinic channels in frog, snake, and tissue cultured chick muscle, respectively. Cull-Candy and Parker (1982) have analyzed the flicker kinetics in glutamate-activated channels in locust skeletal muscle. In the above analyses, the flickers were assumed to represent rapid interconversions of the channel between the doubly liganded open and closed states, thus allowing estimation of channel opening, closing, and agonist dissociation rates.

We have examined the nicotinic channel current during flickers in chick cultured skeletal muscle, and have found that the current, during at least 15% of all flickers, is measurably different from zero (defined as the conductance during long closed periods adjacent to a burst of activity). Thus, a second open state, similar to the one that has been described in rat muscle (Hamill and Sakmann, 1981), must be introduced to account for at least some of the flickers, and the analysis of all flickers, according to the four state sequential model described above, is not valid. Additionally, we have determined that this subconductance state does not necessarily precede channel opening.

METHODS

Chick pectoral muscle from 12–13-d embryos was dissociated with 0.1 mg/ml type I collagenase (Sigma Chemical Corp., St. Louis, MO) in divalent cation-free saline. The cells were grown 4–14 d at 37°C in Dulbecco's modified Eagles medium supplemented with 2% chick embryo extract, 10% heat inactivated horse serum (Gibco Laboratories, Grand Island, NY), penicillin, and streptomycin. Except where noted, we added 1% dimethylsulfoxide (DMSO) to the growth media in order to inhibit fibroblast growth and cause the cells to become rounded.

Electrical recordings were made with a patch system similar to that described by Hamill et al. (1981). For most experiments, we used a Burr-Brown OPA-101 (Burr-Brown Research, Corp., Tucson, AZ) for the head stage amplifier, with an Eltec 10 GΩ resistor (Eltec Instruments, Inc., Dayton Beach, FL) (in parallel with 50 fF stray capacitance) for feedback. Following frequency compensation with two differentiators, the amplifier had a 3-dB frequency response >10 kHz. Spectral analyses of

system noise showed that in the range of 10–300 Hz the power spectral density was 3–4 $\times$ 10^{-30} A^2s. At higher frequencies the power increased with frequency so that at 4 kHz, the power spectral density was ~10 times that at 300 Hz. In some early experiments, we used an uncompensated amplifier (515 with a 1 GΩ feedback resistor; Analog Devices Inc., Norwood, MA), which had a bandwidth of 3.3 kHz. The results with this amplifier were similar to those obtained with the frequency compensated, higher bandwidth version.

Patch pipettes were made from flint glass (100 lambda Drummond Microcaps; Drummond Scientific Co., Broomall, PA) on a standard two stage horizontal electrode puller, which was adjusted to pull electrodes with ~1-μm tip diameter. After being filled, the pipettes were dipped in a hydrophobic molten wax (Kroenig's cement; A. H. Thomas Co., Philadelphia, PA) to decrease pipette noise. Most records were made with the patch attached to the cell. Seal resistances ranged from 2 to 60 GΩ. Transmembrane potentials of the patch ranged from the cell resting potential to 130 mV hyperpolarized from rest giving unitary currents of 1.2 to 7.9 pA. Agonists, acetylcholine (ACh) 50–250 nM, and carbamylcholine (CCh) 50 μM, were dissolved in the pipette filling solution, which consisted of normal saline (without DMSO): 140 mM NaCl, 4 mM KCl, 2 mM CaCl, 1 mM MgCl, and 10 mM HEPES, pH 7.4. Except where noted, the bath solution was growth media containing DMSO supplemented with 10 mM HEPES, pH 7.4. The temperature was 21–24°C.

The data were stored on analog magnetic tape (Racal-Milgo, Inc., Miami, FL). For processing, the data were passed through a four-pole, Bessel response filter (with a cutoff frequency, f_c of 5–10 kHz) and were digitized at the Nyquist frequency. We sometimes invoked a nonrecursive finite impulse response (FIR) digital filter to further limit the bandwidth of the data (Peled and Liu, 1976). The filter approximated the transfer function of an ideal low pass filter using a finite number of terms that were Hamming-tapered to reduce ringing. The number of coefficients varied with the ratio of the desired cutoff frequency to the sampling frequency and was typically 10–30. The bandwidth of the analyzed data ranged from 3–10 kHz.

The records of patch current were analyzed by an automated pattern recognition program (Sachs et al., 1982). Briefly, events were accepted for analysis only if they met certain criteria. First, putative channel currents had to be larger than half of the open channel current. Transition locations were defined by the time at which the events crossed half amplitude. Then bursts, defined as a series of equal amplitude events separated by times less than some arbitrary cutoff (typically 2.5 ms), were compared with an ideal binary burst. The root mean square (rms) deviation of the putative burst from the idealized burst was computed and the burst was accepted for further analysis only if this deviation was less than some threshold value, typically twice the deviation of the baseline noise. Third, the amplitude of the putative burst had to be within a window of current (typically 0.5–1 pA) centered about the single channel current estimate. In addition, all events that contained more than one channel open simultaneously were rejected from further analysis. Channel activity was generally low so that the probability of being closed was >0.85 and the probability of having more than one channel open at a time was <0.01. Once set, the parameters governing the detection criteria remained fixed for the entire record and all of the data were accepted or rejected from further analyses on the basis of these criteria alone.

Because of the threshold crossing criterion, we only analyzed flicker events that were smaller than one-half the unitary current amplitude. Flicker duration was defined as the time spent below threshold. The most difficult measurements were those of the current amplitude during flickers. We only analyzed the amplitude of flickers after allowing the amplifier-filter combination to settle to within 2% of its final value. With sampling at the Nyquist frequency, this meant waiting two or three sample points following threshold crossing before making an amplitude measurement. A similar settling period was applied to those points preceding the subsequent opening transition since multipole filters, digital or analog, have a finite delay. For example, a four-pole Bessel response filter has a delay of $0.336/f_c$ in the step response from the transition to half amplitude. For 8-kHz bandwidths, these constraints limited our analysis of amplitudes to flickers longer than 250 μs. Because duration measurements were less demanding, we could measure durations as short as 100 ms with negligible error.

Curve fitting was done by a nonlinear, least squares algorithm that does not require analytical derivatives (ZXSSQ, from International Mathematical and Statistical Libraries, Inc., Houston, TX). To eliminate the effects of finite bin widths in histogram data, the histograms were fit to integrals of the appropriate probability density functions taken over each bin. The squared residuals calculated by the curve fitting program were weighted inversely with the expected variance, which, in the case of counting statistics, can be well approximated by the variance of a Poisson distribution whose mean is the expected number of counts in a bin (Bevington, 1969). Where quoted, confidence limits on parameters represent conservative support plane estimates at the 90% level. These are confidence limits on a given parameter irrespective of the value of the other parameters (Marquardt, 1964).

RESULTS

Fig. 1 shows an example of a burst initiated by CCh where the data have been filtered at two different bandwidths. With a 1-kHz bandwidth, the flickers are incompletely resolved and their amplitudes are uncertain. With the 8-kHz bandwidth, one of the flickers can be seen to go to a current level distinctly greater than the baseline current. The shorter duration events are still incompletely resolved. The initial opening and the final closing events appear to arise from, and return to, the baseline conductance level.

Flicker durations are distributed as two exponential functions. An example for CCh activated channels is shown in Fig. 2, where the characteristic time constants are

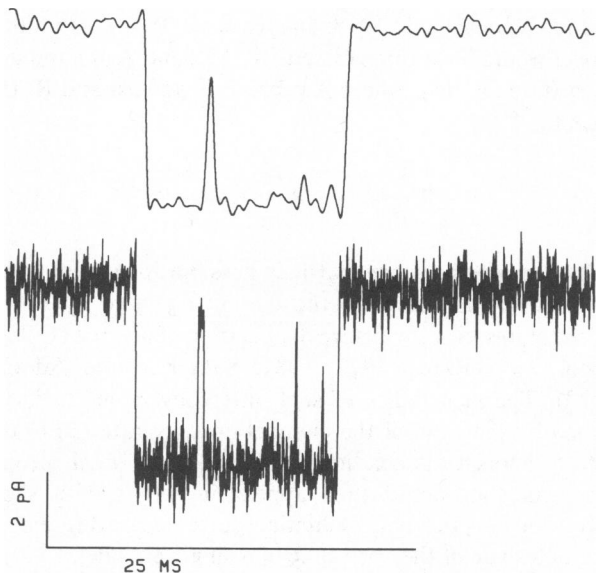

FIGURE 1 An example of a burst of channel activity containing three obvious flickers. Inward current is shown downward. The upper trace shows data filtered at 1 kHz with a linear phase, FIR digital filter (following digitizing at 20 kHz with a four-pole Bessel response filter set to 10 kHz). The lower trace shows the same event with the digital filter bandwidth raised to 8 kHz. The long duration flicker does not appear to reach the baseline. The amplitude of the two shorter events toward the right seems bandwidth limited even at 8 kHz bandwidth used in the lower trace.

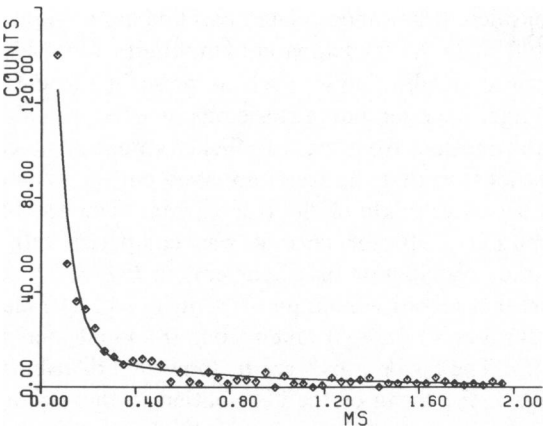

FIGURE 2 Histogram of the duration of flickers from one experiment. The solid line is a nonlinear regression to a sum of two exponentials. The two time constants were 0.08 and 1.03 ms. Due to bandwidth limitations, we did not measure many amplitudes belonging to the fast component, and our data primarily represent an analysis of the slower component (22°C, CCh).

0.080 ± 0.034 and 1.03 ± 0.55 ms. Because of the aforementioned instrumental limitations, our analysis of flicker amplitudes is dominated by the longer of the two distributions. This slower component accounted for ~30% of all intraburst closed periods.

Data such as that in Fig. 1 are suggestive but cannot be convincing because of the presence of overlapping, uncorrelated noise and uncertainty about the amplifier's response time. The problem of random scatter in the data can be overcome by averaging over enough events. The problem of amplifier settling, however, cannot be removed by averaging, and this source of error was our first concern.

As an internal measure of our system response time, we aligned the leading and trailing edges of all bursts, respectively, and averaged them. One such averaged pair is shown in Figs. 3 *a* and *b*. The leading edge of the burst comes squarely out of the baseline and is followed by a decay phase. The decay phase is produced by a decrease in the number of channels open at any given time following the opening transition. The trailing edge of the burst has a similar appearance, with the exception that the settling time to the baseline is more visible. A rapid component of closure visible in the averaged transitions is due to a population of short-lived channels (time constant ~0.2 ms) which often appeared as isolated events. The relative proportion of these short openings to the dominant, longer openings (time constant, 1–15 ms) was variable from one preparation to another, but generally was <10%.

Whatever the settling characteristics of the amplifier, the same dynamics would apply to recordings of flickers and bursts. The results from one patch are shown in Fig. 4, where we have superimposed the mean amplitude of flickers as a function of their duration upon the averaged trailing edge of bursts. The trailing edge is shown from the

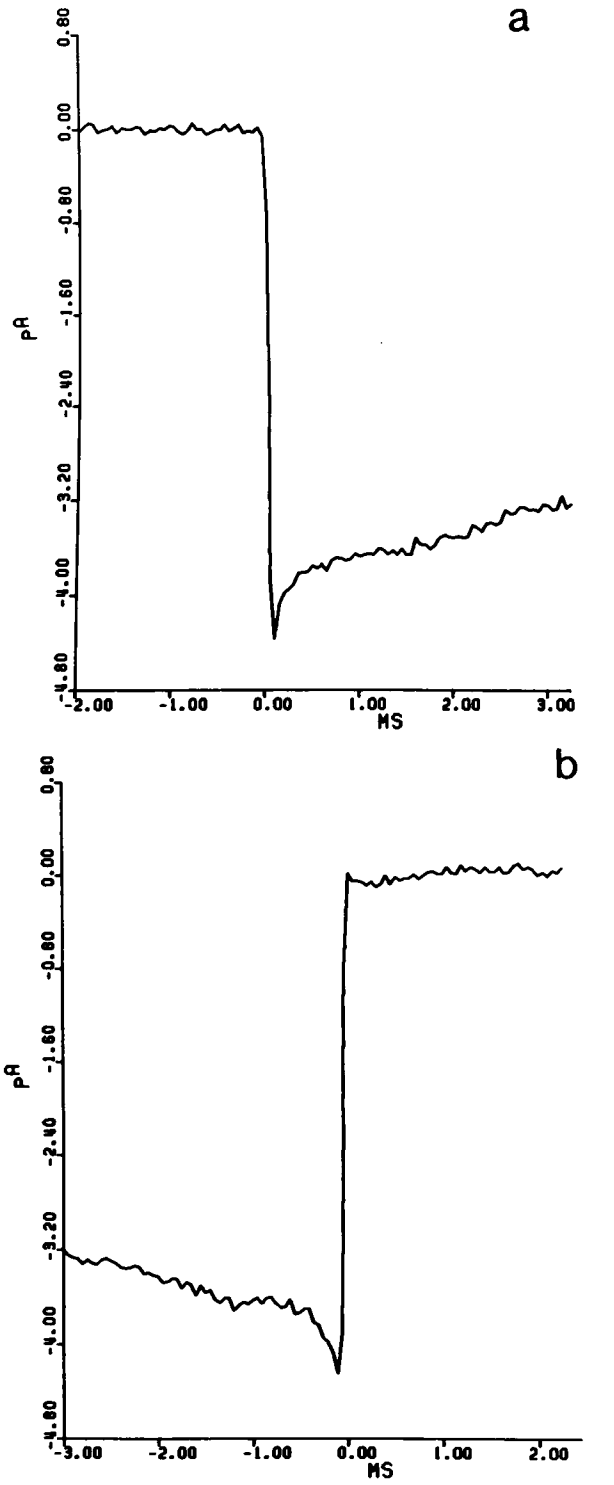

FIGURE 3 Averaged leading (*a*) and trailing edges (*b*) of 313 bursts from one experiment. Bursts were aligned at the moment of threshold crossing. Notice the clean departure of the leading edge from the baseline indicating that on the average, bursts opened directly from the baseline. The decay from the peak current represents the decay in the number of channels open as a function of time. The two phases of decay represent two populations of (full amplitude) open times. The trailing edge record shows some filter and amplifier ringing following return to the baseline. This mean falling phase is used as a response time reference in Fig. 4. (CCh, 22°C).

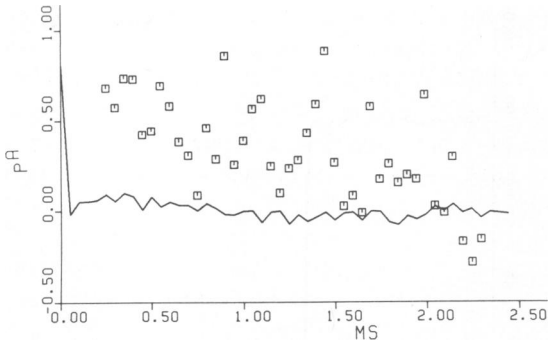

FIGURE 4 Mean amplitude of flickers longer than 250 μs (symbols) plotted as a function of duration (inward current shown upward). Each data point represents the grand mean at each duration. The averaged burst trailing edge (Fig. 3 *b*) is superimposed for reference. As can be seen, the flickers are consistently above baseline for short events, tending toward baseline as they get longer (22°C, CCh).

first point below threshold (one-half amplitude) onward in time. The burst settles quickly relative to the duration of the flickers. Thus amplifier settling cannot account for the finite current flow during flickers. The lack of samples between the origin and 250 μs represents the time allowed for flickers to settle to final amplitude, and as is apparent from the record, the time allotment is conservative.

Because the flickers often appeared to reach current levels that were within the noise envelope of the baseline, we considered that uncorrelated baseline noise might give rise to flickers that had apparent amplitudes >0. Additive, symmetric baseline noise, such as noise in the current-to-voltage converter and intrinsic pipette noise, would both add and subtract from the true flicker amplitude in equal proportions, so that the mean observed current should be an unbiased estimate of the true current. The amplitude distribution of flicker current was compared with the amplitude distribution of all currents in Fig. 5. The data represent a record containing 313 flickers of sufficiently long duration (>250 μs) taken from 784 bursts activated by CCh. The histograms were fit to normal distributions. In Fig. 5, the mean of the distribution in the vicinity of baseline (our zero current reference level) was 0.00 ± 0.02 pA (mean ±90% confidence limit on the mean), the mean of the distribution about the main conductance state was 4.82 ± 0.05 pA, and the mean of the distribution during flickers was 0.33 ± 0.04 pA, or ~7% of the single channel current level. This value is a mixture over all events, some of which reached the baseline and others which did not (see below). Because the average flicker current was greater than that of the baseline, overlapping, symmetrical baseline noise cannot explain the difference.

Asymmetric components of the baseline noise, such as could arise from small, unresolved, channel currents could also bias the estimates of flicker amplitude. For example, small inward currents might sum with flickers to give

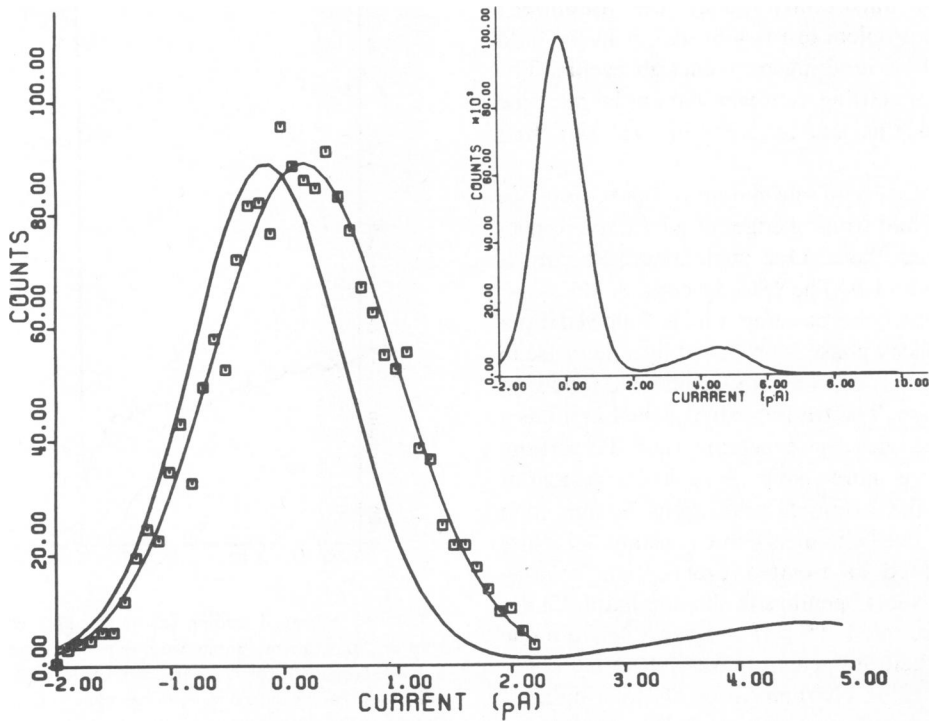

FIGURE 5 Amplitude distribution of all data points from flickers longer than 250 μs (symbols and thin line Gaussian distribution), compared with the baseline amplitude distribution, (thick line is the raw data). The inset shows the amplitude distribution of the entire record from which the baseline distribution of the main panel was taken. The units of the ordinate of the main panel refer to the counts per bin for flickers only. The mean of the flicker amplitude distribution is different from the mean of the background distribution with better than 99.99% confidence (22°C, CCh, bandwidth 8 kHz).

apparent amplitudes above the baseline. To look for low current channels, we analyzed the data with restricted bandwidths (100–250 Hz) so that channel currents <0.3 pA could be detected. In most, but not all, of our records small inward currents were visible. These currents may have been low conductance state(s) of nicotinic channels, nicotinic rim channels located under the sealing region of the patch, or other species of channel.

To eliminate the influence of these subthreshold events, we compared the average amplitude of closing transitions in flickers and bursts. Subthreshold events should cause similar offsets in both classes of events, and the remaining difference can be attributed to differences in transition amplitude.

The mean flicker closing transition and the mean burst closing transitions are compared in Fig. 6. For this comparison, we only averaged events that had no other transitions within the settling time allowance. Consequently, the rapid component of channel closing, as seen in Fig. 3, is suppressed. The difference in transition amplitude between flickers and bursts is apparent. At 150 μs after crossing threshold, the average flicker closing transition is 4.22 pA and the burst termination transition is 4.75 pA. Note that in this form of the data, no data points need to be omitted to allow for settling because the settling dynamics are contained in the figure. Because it is a comparison of two types of closing and hence immune to biases from unresolved channels and overlap of baseline noise, these data are conclusive in showing the existence of a finite current during some flickers.

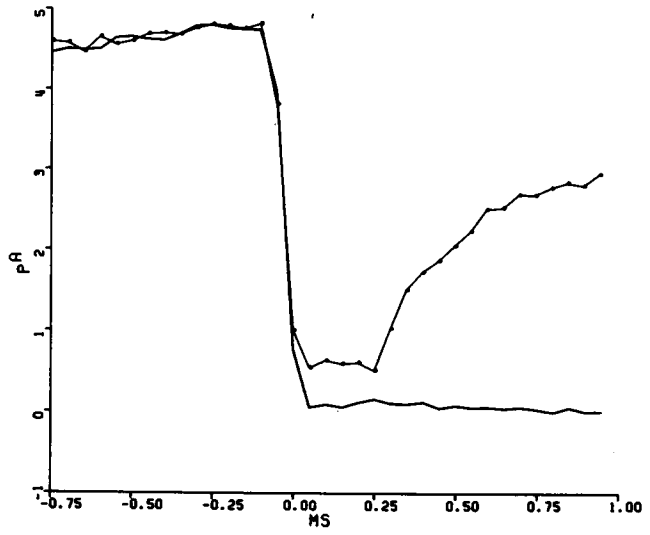

FIGURE 6 The averaged flicker transition (connected symbols) superimposed on the averaged burst trailing edge (solid line), taken from the same record as Fig. 5 (inward current is shown upward). Only events that were both longer than 250 μs and preceded by open times >250 μs in duration were included in the averages. From the flicker state, the average current rises towards the mean current of the burst. If longer times were included, the average would eventually decay to the mean current of the entire record. In this experiment, the average flicker transition was 11% less than that of the average burst termination.

Neither the amplitude distribution of flicker current nor the average flicker transition amplitude gives a complete and accurate estimate of flicker amplitudes. The total amplitude distribution is biased in the sense that longer events contribute more points to the histogram, and longer events tend to have lower current (see below). The mean flicker transition, on the other hand, gives no information on the distribution of flicker amplitudes. In an attempt to circumvent these limitations, we made a cross correlation analysis of mean flicker amplitude with flicker duration on an event-by-event basis. The data from a single record are shown in Fig. 7. In this plot, each symbol represents the mean amplitude of the data points (excluding the settling time) in a single flicker. Most of the flickers had mean amplitudes >0. There is a substantial scatter in the amplitude and the scatter decreases with time (duration). This decrease in scatter is largely due to the number of points used to form the average amplitude. That is, the first data column represents the average amplitude as represented by a single sample. The second column represents the average of two samples, and so on. Scatter could arise from three sources: background noise, noise associated with current fluctuations in the flicker state(s), and errors in determination of the baseline. The background noise should be equally additive for all events and should cause the variance of the measured amplitudes to decrease with the square root of the duration (number of data points). As far as noise associated with the flicker state(s), there is some suggestion in the data that the amplitude variance of the flicker state is greater than that of the background (see below). Finally, low frequency variations in the baseline can contribute variance even for long closed periods. Our analysis program assumes that baselines are flat when, in

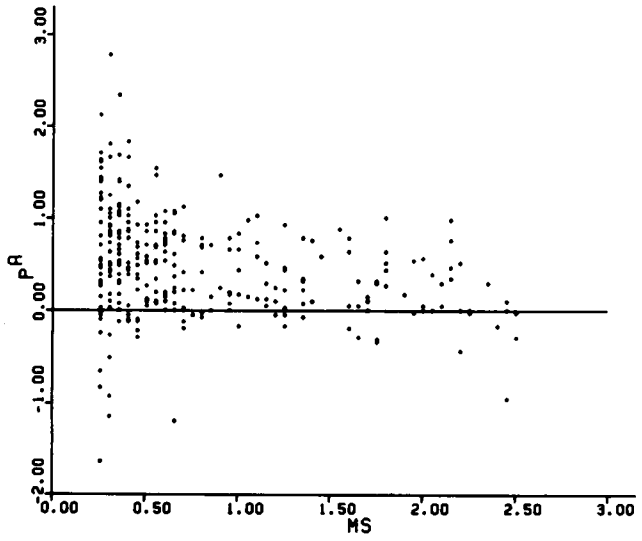

FIGURE 7 Cross correlation plot of mean flicker amplitude vs. duration. Each point represents a single flicker. The decrease of variance with duration is due primarily to the increased number of points forming the means for longer events (22°C, CCh).

fact, there is curvature that contributes to the observed variance.

To test for quantization of flicker amplitudes, we used the amplitude/duration cross correlation data to make histograms of the mean flicker amplitudes. As an example, Fig. 8, taken from the data shown in Fig. 7, shows some clustering at the baseline and in the range of 0.2–0.8 pA (4–17% of the unitary current), but shows substantial spread over other amplitudes. Because of the scatter, the data from any single record were insufficient to detect quantization. To reduce the scatter, we combined data from 11 records, 10 using ACh as the agonist and 1 using CCh as the agonist, all with DMSO present in both the growth and recording media. To account for differences in membrane potential, we normalized the flicker current by the main open state current. Preliminary data (see below) suggest that this normalization is reasonable since the flicker amplitude seems to be a constant fraction of the main state amplitude.

We fit the normalized mean flicker amplitude distribution to a sum of two Gaussian distributions as shown in Fig. 9. The means for the two distributions were at ~0 and 10% of the open state current (Table I). The standard deviation of the population centered at 10% of the open channel current was two to three times greater than that of the zero current population. This difference in variance may reflect the presence of a set of discrete conducting substates centered about the 10% level, or a continuum of states that appear as excess noise. Some of the difference in variance may also arise from differences in duration of states of different amplitude. Zero current flickers are, on the average, longer than the 10% current flickers, hence their mean amplitudes can be measured with greater accuracy and would have a smaller sample variance.

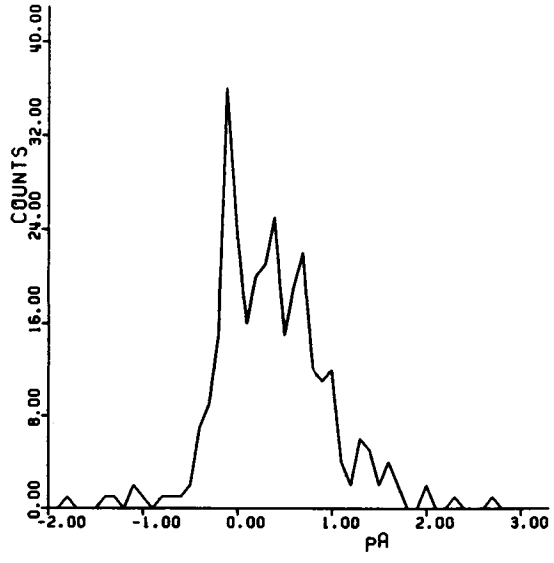

FIGURE 8 Distribution of mean flicker amplitude, taken from the data of Fig. 7. The data appear clustered at baseline (0 pA), and in the range of 0.2–0.8 pA, although it is difficult to place confidence limits on the cluster amplitudes. The single channel current was 4.8 pA.

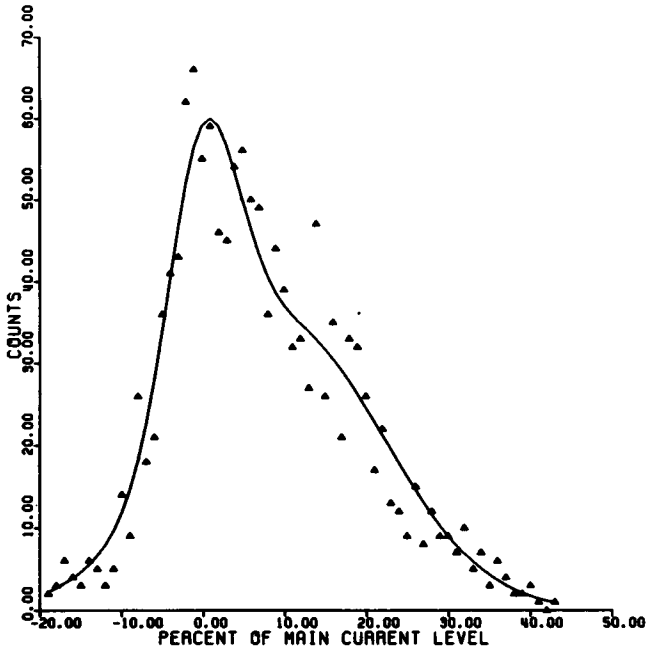

FIGURE 9 Mean flicker amplitude distribution summarized from 11 experiments. Data have been normalized to the current of the main conductance level to permit summarizing over a range of voltages. The data were fit to a sum of two Gaussian distributions (solid line). The distributions are centered at 0 and 9% of the main channel current. (ACh and CCh, 21–24°C, inward currents from 1 to 8 pA.)

Due to the statistical nature of channel opening and closing kinetics, there is a bias in the measurement of flicker amplitudes on an event-by-event basis. After a channel closes, there is a finite probability of the channel reopening and then closing too quickly to be detected. The mean current of that undetected opening will increase the observed flicker current by an amount that depends upon the channel kinetics, the system response time, and the sampling rate (see Appendix). For a worst case estimate, assume that the closing rate is given by the fast component

TABLE I
PROPERTIES OF THE MEAN AMPLITUDE DISTRIBUTION OF FLICKERS

Duration	Mean 1	Mean 2	SD1	SD2	Area 1/ Area 2
ms	%	%	%	%	
0.25–0.75	+0.5 ± 3.9	9.5 ± 3.3	5.1 ± 5.3	12.5 ± 1.9	0.22
0.25–2.5	−0.4 ± 1.7	9.3 ± 2.4	4.3 ± 2.0	12.3 ± 1.3	0.34

Values quoted are taken from nonlinear regressions to a sum of two Gaussian distributions as shown in Fig. 8. Means 1 and 2 refer to the mean flicker amplitude expressed as a percentage of the current during the main conductance state. SD's 1 and 2 are the standard deviations of the two distributions, in the same units, and the relative proportion of population 1 to population 2 is shown in the rightmost column. Error limits are for 90% confidence estimates (Marquardt, 1964).

TABLE II
ESTIMATION OF ERRORS IN OBSERVED FLICKER AMPLITUDES CAUSED BY UNDETECTED OPENING EVENTS

k_c	F_b	F_a	Total
ms^{-1}	%	%	%
5	1.21	0.28	1.49
2	0.48	0.10	0.58
1	0.24	0.05	0.29
0.2	0.05	0.009	0.059
0.1	0.03	0.005	0.035

Assuming an exponential system response (t = 0.32 ms), a sampling interval of 0.1 ms, a channel opening rate (k_o) of 10/ms, and the channel closing rate (k_c) indicated in the Table, F_b represents the amount of current (as a fraction of the open channel current) contributed by events that do not reach threshold. F_a is the fraction contributed by events that are above threshold only in between samples. Total = $F_a + F_b$.

of closing, k_c = 5/ms, and the opening rate is given by the fast component of opening, k_o = 10/ms. Taking the sampling interval as 0.1 ms and the system bandwidth as f_c = 5 kHz, the amplitude contribution of unresolved openings is <1.5% of the open channel amplitude (Table II). A more realistic estimate, obtained by using a 10% contribution of the short open times and a 90% contribution of the long open times (k_c = 0.2/ms), gives an amplitude contribution of <0.2%.

Because some records showed a tendency for longer flickers to have lower mean amplitudes (Figs. 4 and 7), we also examined the distribution of the two populations of flickers as a function of their duration. Using the lumped data set of Fig. 9, we compared the distribution of flicker amplitudes from flickers <2.5 ms in duration to those flickers that were <0.75 ms in duration. In both cases, the amplitude data could be fit to the sum of two Gaussian distributions, one at zero current and one at ~10% of the main current level (Table I). Thus, we conclude that flickers consist of at least two states at all measured times. The proportion of zero-current events increased for shorter events, suggesting that the zero-current population tended to be longer than the 10% current population.

To determine whether the presence of DMSO, either in the growth media or in the recording media, had any effect on flicker amplitude, we did experiments where the cells were grown in normal media without DMSO and in which, before recording, the growth media was exchanged for the saline that we used to fill our patch pipettes. In these experiments we observed flickers with a current level about one-third of the unitary current and others with zero current.[1] In one record (521 sufficiently long flickers from 760 bursts) the average amplitude of a flicker closing transition was ~14% less than the average burst closing transition (2.84 pA). Thus, the finite current during flickers is not DMSO induced, and in fact, the amplitude of the flickers appears to be decreased in the presence of DMSO.

As an independent test of the generality of the finite conductance flicker state, we applied our methods to flicker events produced by the quaternary local anesthetic, QX-222. Previous results indicated that in frog muscle, flickers produced by QX-222 have currents that are <5% of the unitary current (Neher and Steinbach, 1978), but it has recently been suggested that endplate channels blocked by QX-222 have a nonzero conductance (Ruff, 1982). In the experiment whose results are shown in Fig. 10, the interval histogram of flicker durations was distributed essentially as a single exponential with a characteristic time constant of 0.45 ms. A comparison of the number of detected flickers per burst with QX-222 present (6.4) with that in control experiments (0.1–0.8) indicates that most of the flickers that we analyzed were produced by QX-222. We fit the amplitude distribution of flickers to the sum of two Gaussian distributions. The mean of the dominant (QX-222 induced) component of the distribution was 0.062 ± 0.032 pA, or ~1.6% of the open channel current (3.99 pA). Because errors of this magnitude can be caused by current from unresolved events and from residual

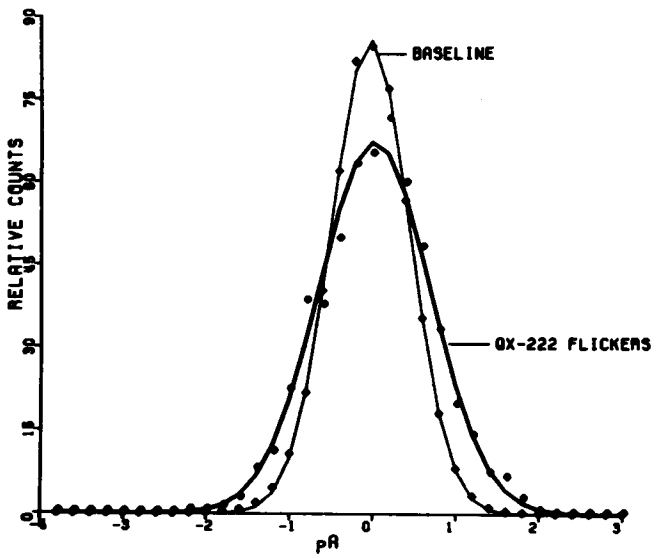

FIGURE 10 Amplitude histogram of the baseline and flickers observed in the presence of QX-222. The data are from 214 flickers within 37 bursts of average amplitude, 3.99 pA. Flicker current (solid symbols) and baseline current (open symbols) were each fit to Gaussian distributions (thick and thin line, respectively). The mean of the flicker current distribution is 1.6% of the open channel current and is statistically indistinguishable from zero. The variance of the flicker current distribution is greater than that of the baseline because data blocks containing long bursts contain relatively less baseline than those with little activity, hence the baseline estimates, although unbiased, have greater scatter. (10 μm QX-222, 150 nM ACh, no DMSO present, 22°C, bandwidth 5 kHz.)

[1]Multiple conductance states in embryonic chick muscle nicotinic channels have also been reported by L. D. Chabala, H. A. Lester, and R. E. Sheridan in *Soc. Neurosci. Symp.* 8:498*a*. (Abstr.).

amplifier settling, we conclude that QX-222 flicker current cannot be distinguished from zero.

DISCUSSION

Because of the short duration of the events and the small currents associated with the flickers, we were skeptical that the results were influenced by amplifier or analysis artifacts. We satisfied ourselves that amplifier settling could not account for the flicker amplitude/duration correlation by examining the averaged falling phase of bursts (Fig. 4). The averaged falling phase, with some rounding due to filtering, was damped and did not decay at the same rate as did flicker amplitude. Additive baseline noise, either symmetric or asymmetric, does not produce flickers with measurable currents, because the mean current during flickers is greater than the mean baseline current (Fig. 5) and the average amplitude of flicker transitions is less than that of a burst terminations (Fig. 6).

The analysis of flicker mean amplitudes on an event-by-event basis from the combined data set (Fig. 9) indicates that about two-thirds of all flickers longer than 250 μs have a current that is, on the average, 10% of the open channel current. The remaining flickers have zero current. One explanation is that the zero-current events were in fact true interburst closed periods. This explanation is unlikely because an examination of the mean flicker amplitudes as a function of duration (Table I) shows that the means of the two amplitude distributions remain constant. Thus even for flicker durations as short as 250–750 μs there are two amplitude populations. Since a duration of 750 μs is short compared with the hundreds of milliseconds between bursts, we conclude that the same channel can produce two flicker amplitudes. Therefore our data suggest that there are at least three short-lived states to which a full open channel can exit. Normalized to the area under the closed time histogram, 75% of the events belong to a population having a time constant of 80 μs and an undefined amplitude(s), 15% of the events belong to a population having a time constant of 1 ms and an amplitude 10% that of the main state, and 10% of the events belong to a population having a 1-ms time constant and an amplitude of zero.

An can be seen from Table I, the population of flickers that has a mean current 10% of the open state also has a standard deviation that is two to three times as great as the zero current flicker state. One might imagine that an object as large as the nicotinic channel, with five subunits (Kistler et al., 1982), would be somewhat flexible and hence have conformations that could modulate a conducting channel. Preliminary evidence suggests that for the open state, the excess noise of the open channel (over background) is proportional to channel current (A. Auerbach and F. Sachs, unpublished observations). Such a flow modulation may be the source of some of the excess variance asssociated with flickers belonging to the 10% amplitude population. Alternatively, the excess variance may represent the presence of closely spaced, stable, conducting states as reported for gramicidin by Busath and Szabo (1981). Unfortunately, there is enough variance in the mean flicker amplitude data to prevent us from observing quantization on an event-by-event basis.

Different conductance states for a given channel have been observed both in artificial bilayer systems (Latorre and Alvarez, 1981) and recently, in the nicotinic channel in tissue cultured rat skeletal muscle (Hamill and Sakmann, 1981; Trautmann, 1982). In this latter preparation, at low temperatures or in the presence of curare, the subconductance state persists for tens of milliseconds, and can be reached both from the main conductance state and, more rarely, from a zero conductance state(s). Nicotinic channels in the L6 cell line also exhibit finite current flickers with amplitudes ~15% that of the open state at 22°C. (D. W. Tank, unpublished observations).

Changes in conductance imply changes in the portion of the channel structure providing the rate limiting steps to permeation. Consequently, we would expect that substates would have different selectivity properties, as shown for some of the gramicidin subconductance states (Szabo and Busath, 1982). With events as short and as small as the flicker currents reported here, selectivity changes will be difficult to measure. We have made a preliminary attempt to measure the reversal potential of the subconductance state by splitting our summary data set (Fig. 9) into two groups, those with inward currents >4.5 pA and those below. (Assuming a single channel conductance of 35 pS, a reversal potential of 0 mV, and a linear current/voltage relationship, 4.5 pA corresponds to a membrane potential of −129 mV.) We fit the normalized mean flicker amplitude histograms of these sets with a sum of two Gaussian distributions. The means of the distribution of flicker amplitudes from the two voltage groups were statistically indistinguishable, suggesting that the substate current is proportional to the main state current, and thus the reversal potentials were similar. Within the limits of our data, it appears that the reduction in current during flickers is due to changes in channel conductance rather than in reversal potential. For comparison, the reversal potentials of the gramicidin A substates are within 11 mV of the reversal potential of the main state across the alkalai cation series (Szabo and Busath, 1982).

The existence of subconductance states needs to be reflected in models of channel kinetics. Our evidence suggests that the fully open state of the channel is usually reached from a zero conductance state, since the averaged leading edge of bursts shows a clear rise from zero with no evidence of a passage through a subconductance state (Fig. 3 *a*). From the variance of the averaged data preceding channel opening, we estimate that the probability of opening from the subconductance state is <0.1. Because of amplifier settling, we cannot set useful limits on the probability of observing the subconductance state following burst termination.

Although the generality of flickering to subconductance states remains to be determined, the similarity of the flickers shown in Fig. 1 to those reported by Nelson and Sachs (1979), Dionne and Leibowitz (1982), Colquhoun and Sakmann (1981), and Cull-Candy and Parker (1982) leads us to suspect the validity of their collective assumption that all flickers represent transitions to a closed, doubly liganded state (A_2R) that precedes channel opening. Alternatively, if none of the flickers represent transitions to the A_2R state, then the burst length represents the inverse of the usual channel closing rate (α) (provided that the time spent in the flicker state is short compared with the time spent in the main conductance state). In this case, the number of events per burst will increase with burst length simply because there is more time for flickers to occur. The number of events per burst would not determine burst length, but rather would be a consequence of burst length. In our experiments, however, most detected flickers were too short for us to accurately measure their amplitudes. These short closings may indeed represent transitions between the doubly liganded open and closed forms of the channel. If so, the kinetic constants calculated from an interpretation of flickers according to the four state sequential model (Eq. 1) would be essentially correct.

APPENDIX

Contribution of Undetected Openings to the Observed Amplitudes of Flickers

During any closed period, there is a finite probability that the channel will open for a time too brief to be detected. The current passed during that opening will contribute to the observed amplitude of the closed period. The extent of this error is a function of the channel kinetics, the frequency response of the system, the sampling rate, and the detection criterion.

The problem can be rephrased in the following way: Given that the channel is closed and the output signal is at threshold at time $t = 0$, what is the mean amplitude at various sample times later, conditional upon not exceeding threshold at any sample points in between? FitzHugh (manuscript submitted for publication) has derived the transition probability density that is conditional upon the starting state and amplitude for a filtered random telegraph signal. His expression for the transition probability density does not directly address the conditional requirement that the channel current be below half amplitude for all points preceding the point in question. Therefore, we have made an approximate solution, which is limited to rate constants in our experimentally observed range.

We will make the following assumptions: the open and closed periods within bursts are distributed as single exponentials, the system response time can be represented by a single time constant, and the system is noise free. We will also ignore the effects of events occurring in earlier sample intervals. By definition, the current must be below half amplitude at the beginning of the interval. At the Nyquist sampling rate, the data points are separated by π time constants, so that the maximum error in amplitude contributed by previous events would be <2%. If we make allowances for settling time from the closing transition, the error is further reduced.

There are two types of missed opening events to consider, those that do not reach half amplitude and those that are above half amplitude only between adjacent samples. The relevant parameters for an exponentially shaped pulse are shown in Fig. 11:

τ is the time constant of the system; T_i is the time from the last sample

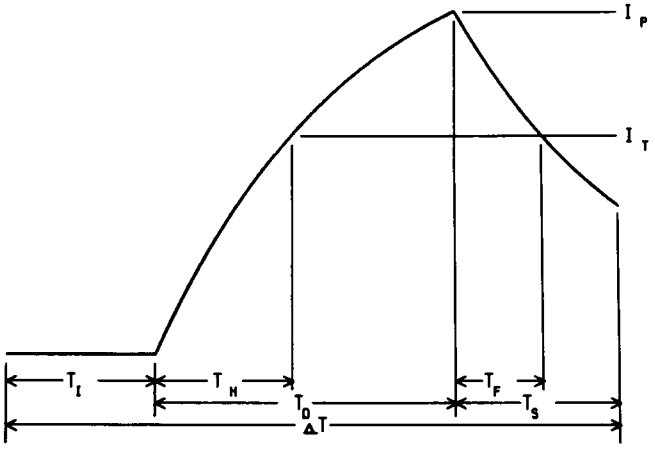

FIGURE 11 An exponentially shaped pulse showing the parameters used to analyze the contribution of unresolved openings to flicker amplitudes. The pulse is drawn to scale for sampling at the Nyquist frequency. See text for details.

to the initiation of a pulse; T_d is the duration of the current pulse; T_h is the time required for the current to reach half amplitude ($= \tau \ln 2$); T_f is the time for the current to fall from peak, I_p, to half amplitude, I_h (only for events longer than T_h); T_s is the time from I_p to the next sample; and Δt is the time between samples.

Consider first the amplitude contribution of those events that do not reach threshold. The mean duration of events not reaching threshold is given by

$$\langle T_d \rangle = \int_0^{T_h} k_c t e^{-k_c t} dt = [1 - e^{-k_c T_h}(k_c T_h + 1)]/k_c,$$

where k_c is the mean channel closing rate. Provided that $\langle T_d \rangle \ll \Delta t$ (see below), the probability of one subthreshold event occurring within time Δt is given by the product of the probabilities for opening within Δt and the probability for being shorter than T_h:

$$P(1) = \int_0^{\Delta t} k_o e^{-k_o t} dt \times \int_0^{T_h} k_c e^{-k_c t} dt = (1 - e^{-k_o \Delta t}) \times (1 - e^{-k_c T_h}),$$

where k_o is the mean channel opening rate. The probability of such events, n, is given by the mean of the geometric probability law, $\langle n \rangle = 1/[1 - P(1)]$, where I_c is the unitary current. The charge transferred by $\langle n \rangle$ events is given by $Q = \langle n \rangle \langle T_d \rangle \langle I_c \rangle$ and the current, expressed as a fraction of the open channel current, passed within a time Δt by $\langle n \rangle$ events of duration $\langle T_d \rangle$ is given by $F_b = \langle n \rangle \langle T_d \rangle / \Delta t$.

The second type of event, that which is above half amplitude only between sample points, produces a different functional form since it is conditional upon being below threshold at $t = 0$ and Δt, and being above threshold in between. For an event such as in Fig. 11, the key parameter is the current at $t = \Delta t$. Now,

$$T_s = \Delta t - T_d - T_i. \tag{A1}$$

The current at $t = \Delta t$ is given by

$$I(\Delta t) = I_p e^{-T_s/\tau}$$

where

$$I_p = I_c (1 - e^{-T_d/\tau}).$$

Substituting from Eq. A1,

$$I(\Delta t) = I_c\,(1 - e^{-T_d/\tau})\,(e^{-(\Delta t - T_d - T_i)/\tau}).$$

The mean of $I(\Delta t)$ is given by integration over the joint distribution of T_i and T_d

$$\langle I(\Delta t)\rangle = I_c \int_{T_d T_h}^{\Delta t - T_f} k_c e^{-k_c T_d} k_o e^{-k_o T_i} \cdot (1 - e^{T_d/\tau})(e^{-(\Delta t - T_d - T_i)/\tau})\mathrm{d}T_i \mathrm{d}T_d.$$

For simplicity, if we let $T_f = 0$ in the upper limit of the inner integral, we have an upper limit on $\langle I(\Delta t)\rangle$. After expanding the integral and performing the integration, the result can be expressed as a fraction of the open channel current, I_c:

$$F_a = \gamma\left(\frac{e^{-T_d C_1}}{C_1} - \frac{e^{-T_d C_2}}{C_2} + \frac{\delta e^{-T_d C_3}}{C_3} + \frac{\delta e^{-T_d C_4}}{C_4}\right)\Bigg|_{T_d - T_h}^{\Delta t},$$

where

$$\gamma = \frac{\tau\, k_c k_o e^{-\Delta t/\tau}}{1 - \tau k_o}$$

$$C_1 = 1/\tau - k_c,$$

$$C_2 = 2/\tau - k_c,$$

$$C_3 = 2/\tau + k_c - k_o, \quad \text{and}$$

$$C_4 = 3/\tau - k_c - k_o.$$

We have estimated the errors in flicker amplitudes contributed by missed openings in Table II for relevant values of k_c. The fixed parameters were $k_o = 10/\text{ms}$, $\tau = 0.032$ ms, and $\Delta t = 0.1$ ms. The mean duration of missed events ranged from 1.1 to 0.03 μs. Given that the open time distribution is made up of $<10\%$ events with $k_c = 5/\text{ms}$ and $>90\%$ with $k_c = 0.2/\text{ms}$, the expected errors are small compared with the observed amplitudes.

Since the above calculation assumed an exponential system response and the absence of noise, we checked the results by analyzing digitally simulated channels with appropriate kinetics and typical signal-to-noise levels. The simulated data were processed through our analysis program, which invoked the digital FIR filter. The error in flicker amplitude was comparable to that shown in Table II.

We would like to thank Jim Neil for programming and conceptual assistance. Chris Lingle and Erwin Neher for helpful suggestions and discussions, and Richard McGarrigle for cell preparation.

This work was supported by the National Institute of Neurological and Communicative Disorders and Stroke (NINCDS 13194).

Received for publication 19 March 1982 and in final form 8 November 1982.

REFERENCES

Bevington, R. P. 1969. Data Reduction and Error Analysis for the Physical Sciences. McGraw-Hill Book Co. Inc., New York.

Busath, D., and G. Szabo. 1981. Gramicidin forms multi-state rectifying channels. *Nature (Lond.).* 294:371–373.

Colquhoun, D., and A. G. Hawkes. 1977. Relaxations and fluctuations of membrane currents that flow through drug operated channels. *Proc. R. Soc. Lond. B. Biol. Sci.* 199:231–262.

Colquhoun, D., and A. G. Hawkes. 1981. On the stochastic properties of single ion channels. *Proc. R. Soc. Lond. B. Biol. Sci.* 211:205–235.

Colquhoun, D., and B. Sakmann. 1981. Fluctuations in the microsecond time range of the current through single acetylcholine receptor ion channels. *Nature (Lond.).* 294:464–466.

Cull-Candy, S. G., and I. Parker. 1982. Rapid kinetics of single glutamate receptor channels. *Nature (Lond.).* 295:410–412.

del Castillo, J., and B. Katz. 1957. Interaction at end-plate receptors between different choline derivatives. *Proc. R. Soc. Lond. B. Biol. Sci.* 146:369–381.

Dionne, V. E., and M. D. Leibowitz. 1982. Acetylcholine receptor kinetics: a description from single channel currents at snake neuromuscular junctions. *Biophys. J.* 39:253–261.

Dionne, V. E., J. H. Steinbach, and C. F. Stevens. 1978. An analysis of the dose-response at voltage-clamped frog neuromuscular junctions. *J. Physiol. (Lond.).* 281:421–444.

Dreyer, F., K. Peper, and R. Sterz. 1978. Determination of dose-response curves by quantitative ionophoresis at the frog neuromuscular junction. *J. Physiol. (Lond.).* 281:395–420.

Hamill, O. P., and B. Sakmann. 1981. Multiple conductance states of single acetylcholine receptor channels in embryonic muscle cells. *Nature (Lond.).* 294:462–464.

Hamill, O. P., A. Marty, E. Neher, B. Sakmann, and F. J. Sigworth. 1981. Improved patch-clamp techniques for high-resolution current recording from cells and cell-free membrane patches. *Pfluegers Arch. Eur. J. Physiol.* 391(2):85–100.

Kistler, J., R. M. Stroud, M. W. Klymkowsky, R. A. Lalancette, and R. H. Fairclough. 1982. Structure and function of an acetylcholine receptor. *Biophys. J.* 37:371–383.

Latorre, R., and O. Alvarez. 1981. Voltage-dependent channels in planar lipid bilayer membranes. *Physiol. Rev.* 61(1):77–150.

Marquardt, D. W. 1964. Least squares estimation of nonlinear parameters. IBM Share Library number 3094. 15–20.

Neher, E., and J. H. Steinbach. 1978. Local anesthetics transiently block currents through single acetylcholine receptor channels. *J. Physiol. (Lond.).* 277:153–176.

Nelson, D. J., and F. Sachs. 1979. Single ionic channels observed in tissue-cultured muscle. *Nature (Lond.).* 282:861–863.

Nelson, D. J., and F. Sachs. 1982. Agonist and channel kinetics of the nicotinic acetylcholine receptor. *Biophys. J.* 37(2, Pt. 2):321*a*. (Abstr.)

Peled, A., and B. Liu. 1976. Digital Signal Processing. John Wiley and Sons, Inc., New York. 67–70.

Ruff, R. L. 1982. The kinetics of local anesthetic blockade of end-plate channels. *Biophys. J.* 37:625–631.

Sachs, F., J. Neil, and N. Barkakati. 1982. The automated analysis of data from single ionic channels. *Pfluegers Arch. Eur. J. Physiol.* 395:331–340.

Sakmann, B., and P. R. Adams. 1979. Biophysical aspects of agonist action at frog endplate. *Adv. Pharm. Chem. Ther.* 1:81–90.

Szabo, G., and D. Busath. 1982. Variation of ion selectivity in the gramicidin A channel. *Biophys. J.* 37(2, Pt. 2):254*a*. (*Abstr.*)

Trautmann, A. 1982. Curare can open and block ionic channels associated with cholinergic receptors. *Nature (Lond.).* 298:272–275.